4th URSI AT-RASC, Gran Canaria, 19-24 May 2024

Microdosimetry of µsPEFs exposure on advanced stem cells 3D models in microfibrils' scaffolds

Sara Fontana*(1,2), Noemi Dolciotti(1), Victoria Moreno-Manzano(3), Lluis M. Mir(4), Franck M. Andre(4), Claudia Consales(5), Francesca Apollonio(1,2) and Micaela Liberti(1,2)
(1) Department of Information Engineering, Electronics and Telecommunications (DIET), Sapienza University of Rome, Rome, Italy; e-mail: sara.fontana@uniroma1.it
(2) Center for Life Nano- & Neuro-Science, Fondazione Istituto Italiano di Tecnologia (IIT), Rome, Italy
(3) Neuronal and Tissue Regeneration Lab, Centro de Investigacion Prıncipe Felipe, Valencia, Spain
(4) UMR 9018 METSY, CNRS, Université Paris-Saclay, Gustave Roussy, Villejuif, France
(5) Division of Health Protection Technologies, ENEA, Rome, Italy

Abstract

Stem cells-based treatments are offering tantalizing prospectives within neuronal tissue engineering, as a versatile tool to promote nerve regeneration after injuries, such as the Spinal Cord Injury (SCI). In this context, the European project RISEUP aims at SCI regeneration through an Electro Pulsed Bio-hybrid (EPB) implantable device, that will support stem cells in a polylactic acid microfibrils' scaffold. The cells' differentiation in neuronal lineage will be fostered through the application of microsecond pulsed electric fields (µsPEFs), typically used for electroporation-based applications. In this work, a microdosimetric study on a mixture of advanced 3D realistic cells' models, including subcellular structures and internal organelles, hosted in a sparser and a denser microfibrils' distribution is presented. The aim is to quantify the induced electrical quantities and the pore formation dynamics at cellular and subcellular level, to evaluate the biophysical effects induced after µsPEFs stimulation.

1. Introduction

In recent times, significant strides have been achieved in stem cells applications, which are increasingly gaining momentum in breakthroughs within regenerative medicine. One of the potential target is the nervous system, that do not undergo self-regeneration and may lead to enduring functional deficit [1]. This approach has a remarkable potential, since it involves harnessing the stem cells' capacity for transforming into specialized cell types, and their neurodegenerative and neuroprotective properties to help nerve recovery [2]. Nonetheless, the use of biocompatible scaffolds is preferred over the direct stem cells transplantation on the lesion site. Indeed, the scaffolds create a stable environment to prevent cells' death and facilitate their growth, in order for them to migrate to the injury site and recover the damaged tissue [3]. In particular, highly aligned microfibrils' substrates have been discovered to guide axonal growth in the fibers' direction [4]. Many research groups are working on the scaffolds' electric functionalization, which has been highlighted to accelerate the cellular processes [5]. A noteworthy application instance of such technology is the Spinal Cord Injury (SCI), for which the need of permanent therapeutic treatments is priority. In this framework, the European project RISEUP (FET Open of Horizon Europe Program 2020)[1] aims at the SCI regeneration by developing an Electro Pulsed Bio-hybrid (EPB) implantable device. In this case the scaffolds' electric functionalization is achieved using a totally innovative interdigitated and flexible electrodes technology, on which a biocompatible microfibrils' scaffold, made of polylactic acid (PLA), is placed. This technology will host human induced neural stem cells (iNSCs) combined with mesenchymal cells (MSCs), in order to control the cells' differentiation through ultra short (hundreds of µs) and highly intense (kV/m) pulsed electric fields (µsPEFs), as able to cause temporary increase in transmembrane potential (TMP) (i.e. reversible electropermeabilization [6]) that induces calcium oscillations [7]. Due to the PLA electric insulating behavior, the influence of 12 different microfibrils' models, with sparser or denser density, characterized by straight, curved or twisted fibers, on the E-field distribution has been numerically assessed in [8]. In this context, the use of microdosimetric techniques, combined with realistic and advanced computational models, is pivotal for the EPB design optimization, as well as for replicating experimental conditions to forecast or give explanations of the cellular stimulation effects [9]–[11]. This work focuses on the multiphysics implementation and on the numerical 3D-microdosimetry of the cells hosted in the EPB, to estimate the electric (E-) field and pore density (N) induced on the cells' models. Realistic MSCs and iNSCs 3D models, including cellular and intracellular structures, have been built from high resolution confocal microscopy images and imported in Comsol Multiphysics (v. 6.0), recreating a cellular mixture for *in vitro* experiments. The cells' mixture is placed over a sparser and a denser microfibrils' model, presented in [8]. The aim is to assess the influence of the microfibrils' distribution on the stimulation results,

[1] Riseup - Riseup (riseup-project.eu)

considering a different exposure scenario related to possible cells' placement inside the EPB.

2. Mixture of iNSCs and MSCs models inside the EPB

The EPB technology is reproduced in Comsol Multiphysics, as a simulative core of a couple of an active and a ground interdigitated electrodes, embedded in a PLA substrate (see [8]). The microfibrils' numerical models are obtained from real microscopy images and placed over the electrodes' strips. For this study, two microfibrils' models have been chosen: the sparser monolayer (Model 1) and the denser monolayer (Model 2). These models are representative of two possible configurations in different scaffold regions, a sorted and dense one (Model 2) and a sparser one due to the manufacturing process or to the presence of extracellular fluid ECM (Model 1). Thereafter, 3D realistic numerical models MSCs and iNSCs were built. Two MSCs models have been chosen from [12], including cytoplasm, nucleus, and endoplasmic reticulum (ER) compartments. Whereas two iNSCs models were obtained from confocal microscopy images, through an *ad-hoc* and semi-automatic reconstruction procedure [13]. The images were segmented in 3D Slicer software v. 4.11, using automatic and manual tools to differentiate each compartment, colored by different fluorescent dyes, and further optimized. The iNSCs models include cytoplasm, nucleus, ER and mitochondria compartments. Finally, all the cells' models are imported in Comsol Multiphysics and placed over the two microfibrils' models, assuring that the cells are almost in contact with each other (Figure 1) to represent a cell mixture.

3. Multiphysics implementation

The Multiphysics problem is implemented in Comsol Multiphysics by coupling the AC/DC Electric Current (ec) module, to solve the electric problem, and Mathematics module Boundary ODEs and DAEs, to describe the pore formation dynamics. A bipolar μsPEF, with a duration of 25 μs (+15 V input voltage) followed by 25 μs (-15 V input voltage), is applied on the active electrode. The μsPEF stimulus triggers the formation of hydrophilic pores over the cellular membranes followed by cell membrane's conductivity increase, which allows the E-field to enter inside the intracellular environment. The pore formation dynamics is commonly described in literature by the Smoluchowski equation [14]:

$$\frac{dN}{dt} = \alpha e^{(\frac{Vm}{Vep})^2} \cdot (1 - \frac{N}{N_0} e^{-q(\frac{Vm}{Vep})^2}) \quad (1)$$

Where N is the pore density per mm^2 and in which the input variable is the TMP (V_m) computed by the ec module. All the parameters are reported in Table I. A term that considers the membrane's conductivity increasing σ_{ep} is added to the unporated membrane conductivity, as follows:

$$\sigma_m = \sigma_{m0} + N \cdot \frac{2\pi r_p^2 \sigma_p h}{\pi r_p + 2h} \quad (2)$$

where r_p is the pore radius, h is the membrane thickness and σ_p is the pore conductivity [15]. All the dielectric properties assigned are taken from literature [12], [16].

Table 1. Parameters' values for Smoluchowski equation.

Name	Symbol	Value
Equilibrium Pore Density	N_0	$1.5 \cdot 10^9\ m^{-2}$
Electroporation Parameter	α	$5 \cdot 10^{11}$
Characteristic Electroporation Voltage	V_{ep}	258 mV
Electroporation Constant	q	2.46
Pore Radius	r_p	0.76 nm

4. Results

The E-field distribution, at the beginning of the pulse, on cellular cytoplasm and on the xy-plane crossing the cells'

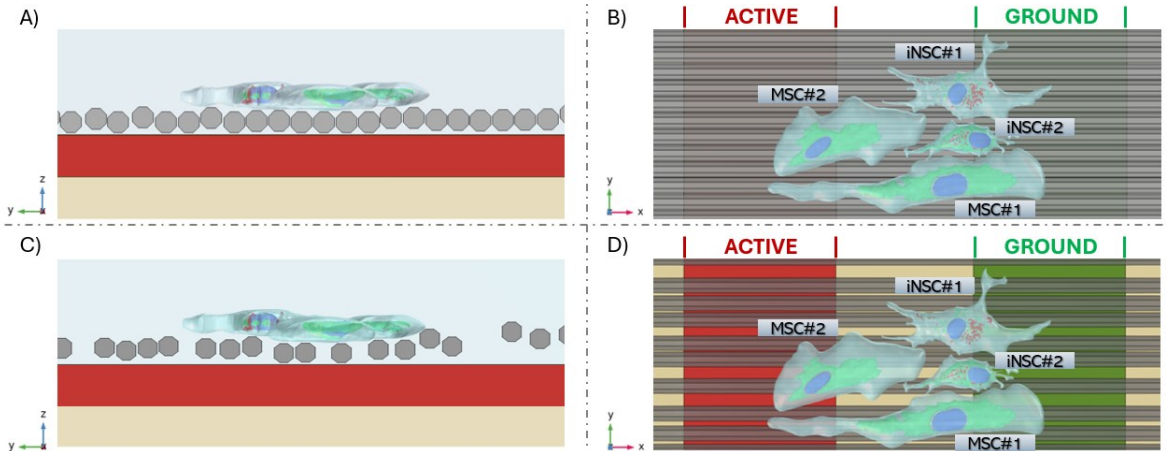

Figure 1. Cross section and the top view of 3D model of the cells' mixture on the microfibrils' dense monolayer (Panel A and B, respectively) and sparse monolayer (Panel C and D, respectively). The cellular compartments are represented considering: cytoplasm in light blue, nucleus in blue, ER in green and mitochondria in red.

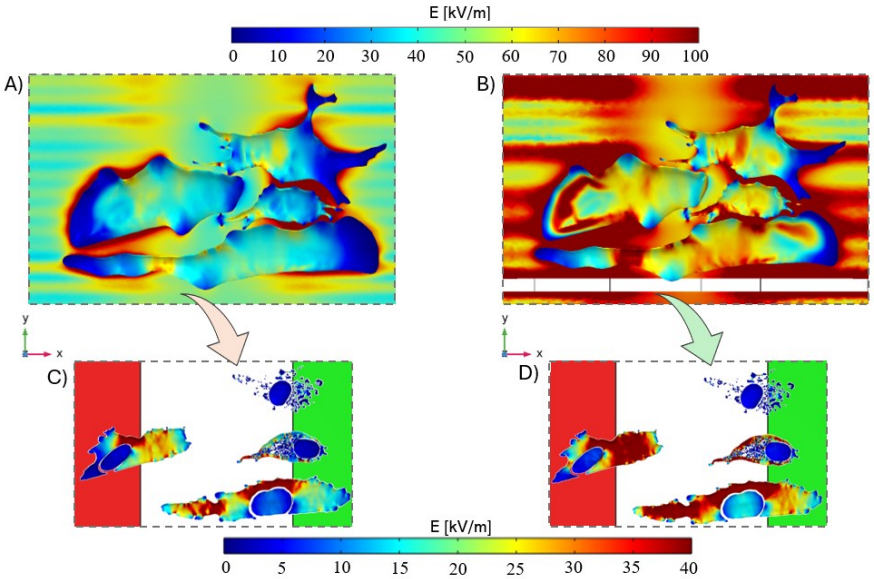

Figure 2. E-field on top view at a quote crossing the center of the cells and on cytoplasm, for the cells placed in denser (panel A) and sparser microfibrils (Panel B). E-field distribution in internal compartments is shown as well in panels C and D at the beginning of the pulse. The electrodes are reported in panels C and D in red and green as a reference.

center, is reported in panels A and B of Figure 2, for denser and sparser microfibrils' respectively. As evident, the E-field distribution in the EPB is influenced by the fibers' spatial density. As discussed in [8] the microfibrils' focuses the field streamlines in the interfibrillar space, creating a bridging effect of the E-field. As expected, in the sparser monolayer (panel B) such an effect is more evident than in the denser one (Panel A), since the fibrils are closer to each other, reducing the focalization effect and thus the cells' exposure. Furthermore, the vicinity of cells determines an E-field focusing near the electrodes, with values up to 100 kV/m also following the cells' irregular shape and size. Consequently, the E-field induced in the intracellular compartments is higher (up to 40 kV/m) and distributed in a wider area, when the cells are placed in the sparser microfibrils' scaffold (Panel D) than in the denser one (Panel C). This led to a TMP increasing (data not shown), following the µsPEF application, reaching up to 1 V, which is a favorable condition for the electroporation process. The considerations on the influence of the microfibrils' density are confirmed also for the pore density distribution (Figure 3) for plasma and inner compartments membranes, in a logarithmic scale at the end of the pulse. Adequate N levels (up to $10^{14}/m^2$) are reached over the plasma membranes for the cells in the sparser microfibrils' model (Panel B). Whereas lower N values are induced on the cells in the denser model (Panel A). The overall fraction of porated membrane increases as the scaffold density decreases, due to the E-field bridging effect that can improve the cells' stimulation. The percentage of porated membrane is therefore generally higher for the cells in the sparser scaffold than those obtained for the denser one. As expected, the amount of fraction of porated membrane that reaches $10^{14}/m^2$ is a about 0.9% for MSC #1, 4% for MSC#2, 2% for iNSC #1 and 1.5% for iNSC#2 when the cells are hosted in the dense scaffold. Whereas values of 10% for MSC#2, 4% for iNSC#2, about %3 for MSC#1 and iNSC#1 are reached when they are hosted in the sparser one. Moreover, with regard to the ER membranes, shown in panel C and D, it can be highlighted that larger ER

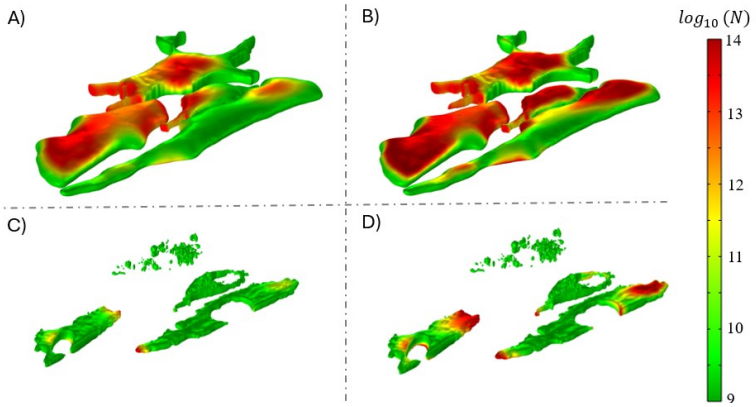

Figure 3. Pore density distribution at the end of the pulse evaluated on plasma membranes (on denser and sparser microfibrils in panel A and B, respectively), on ER membranes and mitochondria membranes (on denser and sparser microfibrils in panel C and D, respectively).

experience higher poration levels. The higher percentage of porated ER membranes are obtained for MSC#1 and MSC#2, respectively equal to 2% and 3% for sparser scaffold and lower than 1% for the denser scaffold. For both cases, despite the sparse scaffold facilitates electroporation, mitochondria don't reach adequate poration levels, probably also due to their uneven and scattered shape.

5. Conclusions

In conclusion, in this work a mixture of advanced and realistic 3D models of iNSC and MSC cells inside the EPB have been used to perform the microdosimetry of *in vitro* experiments. Results have demonstrated the importance of considering different microfibrils' distribution, as inalienable factor influencing the cells' stimulation results. Furthermore, the realistic shape of the cell and its internal organelles are pivotal to perform reliable microdosimetric analysis, to validate or predict experimental results. Finally, stem cells can be electroporated using µsPEF, generated by the electrodes technology proposed within RISEUP for the SCI regeneration.

6. Acknowledgements

This work has been developed in the framework of and supported by the FET-OPEN RISEUP project funded by the European Union's Horizon 2020 research and innovation program (grant agreement No. 964562).

References

[1] R. Boni, A. Ali, A. Shavandi, and A. N. Clarkson, "Current and novel polymeric biomaterials for neural tissue engineering," *J. Biomed. Sci.*, vol. 25, no. 1, pp. 1–21, 2018, doi: 10.1186/s12929-018-0491-8.

[2] H. Ahmadian-Moghadam, M. S. Sadat-Shirazi, and M. R. Zarrindast, "Therapeutic potential of stem cells for treatment of neurodegenerative diseases," *Biotechnol. Lett.*, vol. 42, no. 7, pp. 1073–1101, 2020, doi: 10.1007/s10529-020-02886-1.

[3] Y. Wang, H. Tan, and X. Hui, "Biomaterial Scaffolds in Regenerative Therapy of the Central Nervous System," 2018, doi: 10.1155/2018/7848901.

[4] F. Gisbert Roca, J. Más Estellés, M. M. Pradas, and C. Martínez-Ramos, "Axonal extension from dorsal root ganglia on fibrillar and highly aligned poly(lactic acid)-polypyrrole substrates obtained by two different techniques: Electrospun nanofibres and extruded microfibres," 2020, doi: 10.1016/j.ijbiomac.2020.09.181.

[5] F. Gisbert Roca, S. Serrano Requena, M. Monleón Pradas, and C. Martínez-Ramos, "Electrical Stimulation Increases Axonal Growth from Dorsal Root Ganglia Co-Cultured with Schwann Cells in Highly Aligned PLA-PPy-Au Microfiber Substrates," *Int. J. Mol. Sci.*, vol. 23, no. 12, 2022, doi: 10.3390/ijms23126362.

[6] L. Caramazza *et al.*, "Proof-of-Concept of Electrical Activation of Liposome Nanocarriers: From Dry to Wet Experiments," *Front. Bioeng. Biotechnol.*, vol. 8, p. 552304, Jul. 2020, doi: 10.3389/FBIOE.2020.00819/BIBTEX.

[7] H. Hanna, A. Denzi, M. Liberti, F. M. André, and L. M. Mir, "Electropermeabilization of Inner and Outer Cell Membranes with Microsecond Pulsed Electric Fields: Quantitative Study with Calcium Ions," *Sci. Rep.*, vol. 7, no. 1, pp. 1–14, 2017, doi: 10.1038/s41598-017-12960-w.

[8] S. Fontana *et al.*, "Electric field bridging-effect in electrified microfibrils' scaffolds," *Front. Bioeng. Biotechnol.*, vol. 11, p. 1264406, Oct. 2023, doi: 10.3389/FBIOE.2023.1264406.

[9] L. Caramazza *et al.*, "A microdosimetric study at the cellular and intracellular level using a 3D realistic cell model; A microdosimetric study at the cellular and intracellular level using a 3D realistic cell model," *2021 51st Eur. Microw. Conf.*, 2021, doi: 10.23919/EuMC50147.2022.9784171ï.

[10] A. Paffi *et al.*, "Neuro-functionalized Microdosimetric Models for Applications of Electroporation," *2023 IEEE MTT-S Int. Microw. Biomed. Conf.*, no. 964562, pp. 1–3, 2023, doi: 10.1109/imbioc56839.2023.10304883.

[11] A. Paffi *et al.*, "Electro Pulsed Devices for Regeneration of Injuried Spinal Cord: Advanced Modelling of Microdevices and Cells," pp. 329–332, 2023, doi: 10.1109/iceaa57318.2023.10297845.

[12] A. De Angelis *et al.*, "Confocal Microscopy Improves 3D Microdosimetry Applied to Nanoporation Experiments Targeting Endoplasmic Reticulum," 2020, doi: 10.3389/fbioe.2020.552261.

[13] M. Colella *et al.*, "Patient Semi-specific Computational Modeling of Electromagnetic Stimulation Applied to Neuroprotective Treatments in Acute Ischemic Stroke," *Sci. Rep.*, vol. 10, no. 1, pp. 1–11, 2020, doi: 10.1038/s41598-020-59471-9.

[14] K. A. Debruin and W. Krassowska, "Modeling Electroporation in a Single Cell. I. Effects of Field Strength and Rest Potential," 1999, doi: 10.1016/S0006-3495(99)76973-0.

[15] B. Mercadal, P. T. Vernier, and A. Ivorra, "Dependence of Electroporation Detection Threshold on Cell Radius: An Explanation to Observations Non Compatible with Schwan's Equation Model," *J. Membr. Biol.*, vol. 249, no. 5, pp. 663–676, Oct. 2016, doi: 10.1007/S00232-016-9907-0/FIGURES/5.

[16] Z. HAIDER *et al.*, "Local Dosimetry at Cellular and Subcellular Level in HF and Millimeter-Wave Bands," *IEEE J. Microwaves*, vol. 1, no. 4, pp. 1003–1014, 2021, doi: 10.1109/jmw.2021.3111965.